N91-24066

LOCALIZED CORROSION OF HIGH PERFORMANCE METAL ALLOYS IN AN ACID/SALT ENVIRONMENT

L. G. MacDowell
NASA Materials Science Laboratory
Kennedy Space Center, FL 32899

C. Ontiveros
California State Polytechnic University
Pomona, CA 91768

ABSTRACT

Various vacuum jacketed cryogenic supply lines at the Space Shuttle launch site at Kennedy Space Center use convoluted flexible expansion joints. The atmosphere at the launch site has a very high salt content, and during a launch, fuel combustion products include hydrochloric acid. This extremely corrosive environment has caused pitting corrosion failure in the thin walled 304L stainless steel flex hoses. A search was done to find a more corrosion resistant replacement material. This study focused on 19 metal alloys. Tests which were performed include electrochemical corrosion testing, accelerated corrosion testing in a salt fog chamber, and long term exposure at a beach corrosion testing site. Based on the results of these tests, several nickel based alloys were found to have very high resistance to this corrosive environment. Also, there was excellent agreement between the electrochemical tests and the actual beach exposure tests. This suggests that electrochemical testing may be useful for narrowing the field of potential candidate alloys before subjecting samples to long term beach exposure.

INTRODUCTION

Flexible hoses are used in various supply lines that service the Space Shuttle Orbiter at the launch pad. These thin walled (.025 in) (.064 cm) convoluted flexible hoses were originally made out of 304L stainless steel. The atmosphere at the launch site has a very high chloride content caused by the proximity of the Atlantic Ocean. During a lunch, the products from the fuel combustion reaction include concentrated hydrochloric acid. This combination of chloride and acid leads to a very corrosive environment. This type of environment causes severe pitting in some of the common stainless steel alloys. In the case of vacuum jacketed cryogenic lines, pinhole leaks caused by failure of the flex hose by pitting produces a loss of vacuum and subsequent loss of insulation. An experimental study was carried out on 19 candidate alloys, including 304L stainless steel for comparison. These alloys were chosen on the basis of their reported resistance to chloride environments. Accelerated corrosion testing and actual field tests were performed with the 19 alloys. This paper summarizes the results of these tests.

EXPERIMENTAL PROCEDURE

Materials

The nominal compositions of the 19 candidate alloys are listed in Table 1. As can be seen from the table, alloys A through I are nickel based alloys. Alloy J is zirconium, and alloys K through S are various stainless steels and other iron based alloys. Alloy K is stainless steel 304L, which is the material originally used to construct the flexible expansion joints.

Electrochemical Tests

A Model 351-2 Corrosion Measurement System, manufactured by EG&G Princeton Applied Research, was used for all electrochemical measurements. Specimens were flat coupons 5/8 in. (1.59 cm) in diameter. The specimen holder is designed such that the exposed metal surface area is 1 cm. The electrochemical cell

included a saturated calomel reference electrode (SCE), 2 graphite rod counter electrodes, the metal specimen working electrode, and a bubbler/vent tube. The electrolyte was an aerated solution of HCl plus 3.55wt% NaCl. The concentration of HCl was 0.1N for the first round of testing and was increased to 1.0N for a second round of tests on the more resistant alloys. The solutions were made using deionized water.

Test specimens were polished with 600-grit paper, ultrasonically degreased in a detergent solution, dried, and weighed before immersion in the electrolyte. The electrolyte solution was aerated for at least 45 minutes before immersion of a test specimen. Aeration continued throughout the test. Electrochemical tests performed include determining corrosion potential, polarization resistance, and cyclic polarization. The polarization resistance test procedure was based on ASTM G59. The cyclic polarization procedure was based on ASTM G61. All three electrochemical tests can be run in sequence on a single specimen.

The corrosion potential (Ecorr) was monitored for 3600 seconds, after which time the potential had usually stabilized. For the polarization resistance test, the potential was varied from -20mV to +20mV relative to the measured corrosion potential, while the resulting current was recorded. The scan rate was 0.1 mV/sec. A linear graph of potential vs. current density was made, and the resulting slope (at zero current) plus the Tafel constants were used to calculate the corrosion rate in mils per year (mpy). Tafel constants were calculated using the forward scan of the cyclic polarization data. The cyclic polarization scan started at -250mV relative to Ecorr. The scan rate was 0.166 mV/sec, and the scan was reversed when the current density reached 5 mA/cm^2. The reverse potential scan continued until the potential returned to the starting point of -250mV relative to Ecorr. A graph was then made of potential vs logarithm of current density.

Salt Fog Chamber/Acid Dip

An Atlas Corrosive Fog Exposure System Model SF-2000, manufactured by Atlas Electric Devices Company, was used for accelerated exposure. The solution for salt fog exposure was standard 5% sodium chloride mixture. Specimens were also periodically dipped in a 1.0N hydrochloric acid/alumina mixture. The particles size of the alumina was 0.3 micron. Flat specimens 1in x 2in x 1/8in (2.54cm x 5.08cm x 0.32cm) were used. One set of samples were base metals with an autogenous weld on one end. Another set of samples were the base metal welded to 304L stainless steel. All flat specimens had a 3/8in (0.95cm) hole drilled in the center for mounting purposes. Stress corrosion cracking specimens were also used. These were standard U-bend samples prepared with a weld in the center of the bend.

The flat specimens were weighed on a Mettler AE160 electronic balance. The specimens were then mounted on insulated rods and set in the salt fog chamber at about 15-20 degrees off the vertical. The specimens were exposed to one week of salt fog per ASTM B117. The temperature of the chamber was controlled at 95°F (35°C) . After the one week exposure, the specimens were removed and dipped in the hydrochloric acid/ alumina mixture to simulate the effluent created during launch of the Space Shuttle. After one minute of immersion, the specimens were allowed to drain and dry overnight. The samples were installed in the salt fog chamber for another week, followed by another acid/alumina dip. After a four week/four dip period, the specimens were removed from the mounting rod, cleaned, and weighed. After this inspection, the samples were remounted and returned to the salt fog chamber for another four week/four dip cycle of testing.

Beach Exposure/Acid Spray

All exposure was carried out at the beach corrosion testing site located about 100 feet (30.5m) from the high tide line, along the Atlantic Ocean at Kennedy Space Center, Florida. The metal specimens were a duplicate set as described above for the salt fog/acid dip tests. An acid solution of 10% hydrochloric acid by volume (about 1.0N) mixed with 0.3 micron alumina powder was used. The procedure was based on ASTM G50, with the addition of an acid spray. The specimens were weighed and mounted on short insulated rods that were attached to a plexiglas sheet. The specimens were mounted face side up, facing east towards the ocean at a 45 degree angle and were boldly exposed to the environment to receive the full extent of sun, rain, and sea spray. Approximately every two weeks, the specimens received an acid spray to simulate the effluent during a launch. The acid solution was allowed to remain on the surface of the specimens until it dried or

was rinsed off by rain. Periodically, the specimens were removed from the beach, cleaned, and weighed. The samples were then remounted and returned to the beach for continued exposure and acid sprays.

RESULTS

Electrochemical

The electrochemical tests were run first with 3.55 wt% NaCl and 0.1N HCl, measuring only corrosion potential and cyclic polarization data. These tests were repeated, with the insertion of the polarization resistance experiment. There was very good agreement between the two sets of experiments, indicating good reproductibility and a negligible effect of the polarization resistance test on the cyclic polarization results.

Corrosion Potential. Corrosion potential (Ecorr) gives an indication of how noble an alloy is in a given environment. Figure 1 shows the corrosion potential vs. time data for a stable material. Some materials displayed very unstable corrosion potentials, such as shown in Figure 2. Table 2 shows the results for the 19 alloys tested, in order of increasing activity. The potentials are all with respect to the saturated calomel electrode (SCE) reference and were recorded after 1 hour.

Polarization Resistance. Polarization resistance (R_p) is used to calculate the uniform corrosion rate when the potential is close to the corrosion potential. Results of a typical polarization resistance run are shown in Figure 3. The slope of this line is Rp in ohms. Corrosion current density and uniform corrosion rate are then calculated as follows

$$\text{Icorr} = \frac{106\ Ba\ Bc}{2.3\ Rp\ (Ba + Bc)} \qquad (1)$$

$$\text{Corrosion Rate} = \frac{0.13\ \text{Icorr}\ (E.W.)}{d} \qquad (2)$$

where Ba and Bc are the Tafel constants in V/decade, Icorr is the corrosion current density in A/cm^2, E.W. is the equivalent weight in g/equiv, d is the density in g/cm^3, and corrosion rate is mils per year (mpy). Table 3 summarizes the polarization resistance results, with the alloys ranked in order of increasing corrosion rate. The polarization resistance results did not correlate with beach exposure and salt fog chamber results as well as the cyclic polarization results did. In general, the polarization resistance technique works better with metals that display active corrosion behavior in a given environment. It may not give accurate results for passive metal behavior such as many of the alloys displayed during this study. So, for these. exposure conditions, polarization resistance is not the best electrochemical technique to use to predict actual field exposure corrosion results.

Cyclic Polarization. Cyclic polarization gives an indication of a specimen's resistance to pitting corrosion[1,2], and this method as been used for many systems to determine susceptibility to localized corrosion[1-10]. Figure 4 shows a curve with the hysteresis effect typical of a material with a low resistance to pitting. Since the potential scan is at a known constant rate, the potential values can be converted to time, and the area inside the hysteresis loop can be found by integration to give units of coulomb/CM^2. This area value should be very small for alloys that are highly resistant to pitting, as seen in Figure 5 which is for a material that is very corrosion resistant. In this case, the reverse scan traces almost exactly over the forward scan. Table 4 ranks the alloys according to area of the hysteresis loop. Visual inspection and inspection under a microscope revealed various levels of pitting corrosion. Crevice corrosion was also observed on several of the samples around the edge of the specimen holder. These visual observations agreed extremely well with the electrochemical results. Some alloys displayed uniform corrosion, rather than localized pitting or crevice corrosion. In these instances, the cyclic polarization curves were similar to the one shown in Figure 6. This type of curve does not yield a meaningful value for hysteresis loop area. Therefore, data for this type of

behavior does not appear with the cyclic polarization results.

Increased Acid Concentration. Based on the data in the preceding tables, the most resistant alloys were chosen and run through the same electrochemical tests using a more aggressive electrolyte of 3.55 wt% NaCl with the HCl concentration increased to 1.ON. Stainless steel 304L was also used, as a basis for comparison. Table 5 shows the effect on corrosion potential of increasing the acid concentration. Table 6 shows the polarization resistance results obtained with the higher acid concentration. As with the results in Table 3, this test separates out some of the poor performers, but it can not rank the alloys accurately. The cyclic polarization results for the stronger electrolyte are summarized in Table 7, with the alloys ranked according to weight loss. The 304L sample experienced uniform corrosion. Therefore, results for 304L do not appear in Table 7, for the reason mentioned in regard to Figure 6 (i.e., no meaningful value for hysteresis loop area). Alloys R and Q suffered severe uniform corrosion, in addition to pitting, which is why the area values for these two alloys do not correlate with the weight loss values. Since there was uniform corrosion, the area values are not really meaningful, and the weight loss gives a better indication of the extent of corrosion for these two alloys.

Salt Fog Chamber/Acid Dip

Corrosion rates were calculated by

$$\text{Corrosion Rate (mpy)} = \frac{534\ w}{dAt} \qquad (3)$$

where w is the weight loss in mg, d is the metal density in g/CM^3, A is the area of exposure in in^2, and t is the exposure time in hours. This expression calculates the uniform corrosion rate over the entire surface and gives no indication of the severity of localized attach (pitting and/or crevice corrosion). Specimens were also examined visually for signs of localized corrosion. Table 8 summarizes the weight loss and corrosion rate results after 8 weeks and after 20 weeks. These results are for the autogenous weld samples.

In conjunction with the standard alloy coupons, specimens welded to 304L stainless steel were also tested. This was done since any new replacement alloy would be installed in an existing 304L stainless steel piping system, and galvanic corrosion in the weld area could become a source of system failure. Most of these specimens suffered some type of weld decay. In general, the deterioration was mainly on the 304L surfaces adjacent to the weld. Since the particular application of a new corrosion resistant alloy would be to form thin wall convolutes welded to a heavy wall 304L stainless steel pipe, the galvanic effect should be minimal.

Beach Exposure/Acid Spray

Corrosion rates were calculated using equation 3. The weight loss and corrosion rate data are shown in Table 9 for 60 days, 251 days, and 479 days of exposure. As can be seen from the table, several materials clearly separated from the rest and displayed excellent corrosion resistance. Alloys B, F, C, and A showed virtually no weight loss after more than 15 months on the beach and 30 acid sprays. These are all nickel based alloys. The various stainless steel alloys all showed considerably higher corrosion rates.

CONCLUSIONS

There was excellent agreement between the cyclic polarization results and the long term beach exposure results. With the exception of the zirconium sample (alloy J), which performed quite well at the beach but not under cyclic polarization conditions, the top six alloys from the cyclic polarization tests are the same as the beach exposure results. This supports the claim that cyclic polarization is a good way to determine an alloy's resistance to localized corrosion in a given electrolyte. Cyclic polarization is very quick compared to long term beach exposure. This accelerated test can be used to screen prospective alloys before exposing them to actual beach conditions.

When the beach results are compared to the salt fog results, many materials change positions relative to each other. In general, though, the materials at the top and at the bottom of each list remained in their respective positions. Beach testing should be considered the best judge of alloy's performance since it has naturally occurring conditions. However, the accelerated testing does give insight into which metals have a good chance of performing well.

Finally, several alloys were found that have superior resistance to pitting and crevice corrosion in an acidic salt environment. Alloy B was chosen and has been used to replace some of the thin walled flexible expansion joints at the Space Shuttle launch pad.

REFERENCES

1. ASTM G61-78, Standard Practice for Conducting Cyclic Potentiodynamic Polarization Measurements For Localized Corrosion, 1986 Annual Book of ASTM Standards, Volume 03.02, ASTM, Philadelphia, PA, 1986.

2. R. Baboian, G.S. Haynes, Cyclic Polarization measurements - Experimental Procedure and Evaluation of Test Data, in Electrochemical Corrosion Testing, ASTM STP 727, F. Mansfeld, U. Bertocci, Eds., ASTM, Philadelphia, PA, p. 274, 1981.

3. W. F. Bogaerts, A.A. Van Haute, Corrosion Science, Vol., 25, No. 12, p. 1149, 1985.

4. A. Kawashima, K. Hashimoto, Corrosion Science, Vol 26, No. 6, p. 467, 1986.

5. B.E. Wilde, Corrosion, Vol. 42, No. 3, p. 147, 1986.

6. P.B. Lindsay, Materials Performance, Vol. 25, No. 12, p. 23, 1986.

7. A.I. Asphahani, Materials Performance, Vol. 19, No. 8, P. 9, 1980.

8. R. Bandy, D. Van Rooyen, Corrosion, Vol. 39, No. 6, p. 227, 1983.

9. P.E. Manning, Corrosion, Vol. 39, No. 3, p. 98, 1983.

10. E.L. Liening, Materials Performance, Vol. 19, No. 2, p. 35, 1980

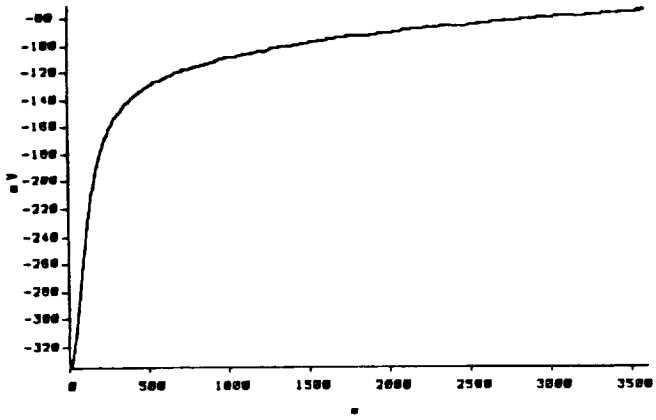

Figure 1 Stable Corrosion Potential
Alloy R in Aerated 3.55%NaCl + 0.1NHCl
Corrosion Potential (mV) vs Time (sec)

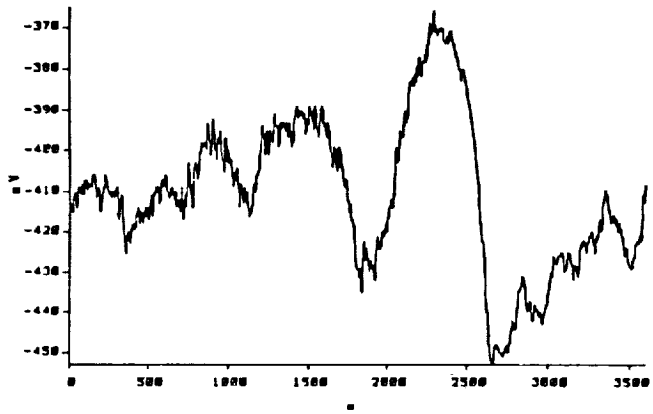

Figure 2 Unstable Corrosion Potential
Alloy L in Aerated 3.55%NaCl + 0.1NHCl
Corrosion Potential (mV) vs Time (sec)

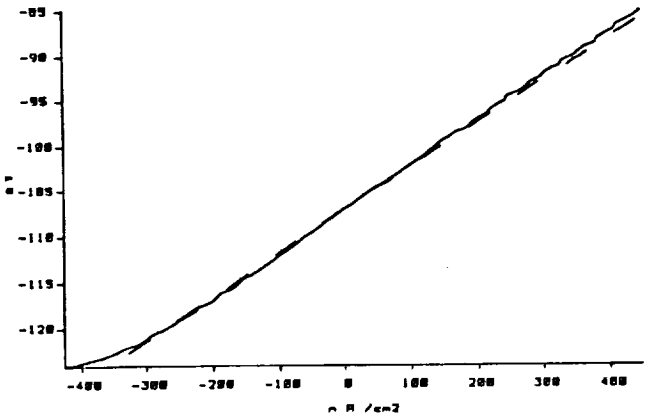

Figure 3 Polarization Resistance Graph
Alloy A in Aerated 3.55%NaCl + 0.1NHCl
Potential(mV) vs Current Density(nA/cm^2)

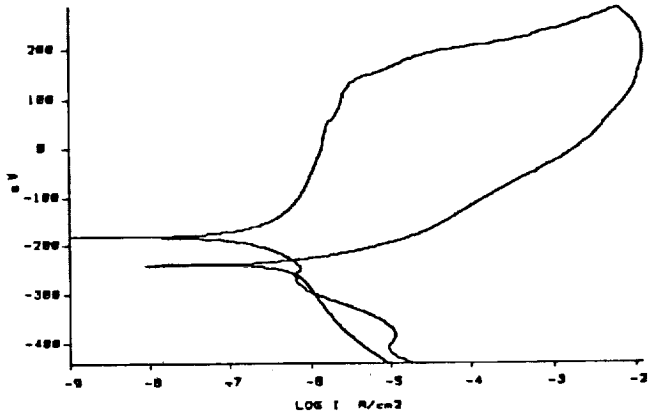

Figure 4 Cyclic Polarization With
Hysteresis Loop
Alloy M in Aerated 3.55%NaCl + 0.1NHCl
Potential (mV) vs log I(A/cm^2)

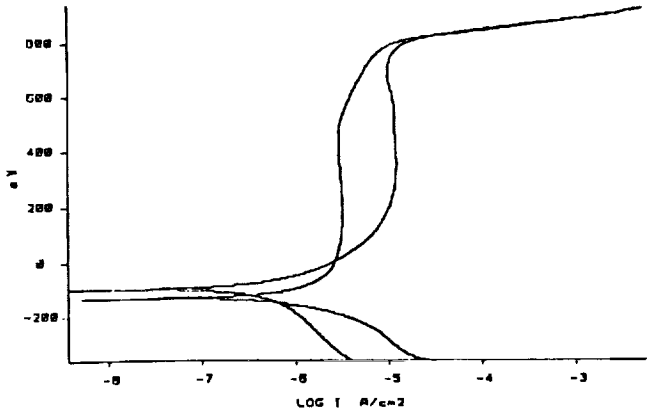

Figure 5 Cyclic Polarization Without
Hysteresis Loop
Alloy A in Aerated 3.55%NaCl + 0.1N HCl
Potential (mV) vs log I(A/cm^2)

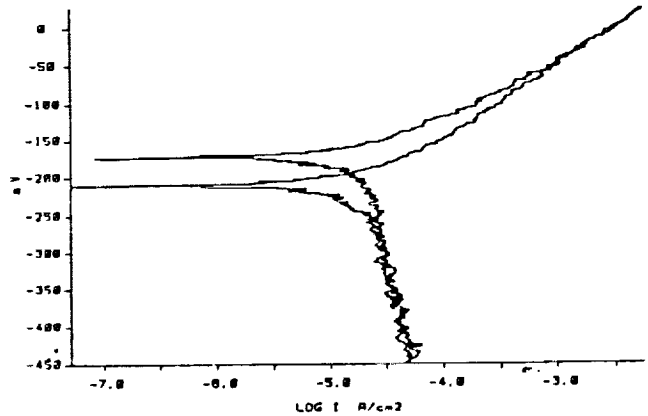

Figure 6 Cyclic Polarization With
Uniform Corrosion
Alloy I in Aerated 3.55%NaCl + 0.1N HCl
Potential (mV) vs Log Current
Density (A/cm^2)

TABLE 1
NOMINAL COMPOSITIONS (WT%) OF THE CANDIDATE ALLOYS

Alloy	Ni	Fe	Cr	Mo	Mn*	Cu	C*	Si*	Other
A	Bal.	3.0	18	17	1.0		.01	.08	
B	Bal.	3.0	22	13	0.5		.01	.08	V 0.3,W 3
C	Bal.	7.0	17	17	1.0		.01	.08	V 0.3,W 4.5
D	Bal.	2.0	1	28	1.0		.01	.10	
E	Bal.	8.0	16		1.0	0.5	.15	.50	
F	Bal.	5.0	23	10	0.5		.10	.50	
G	Bal.	22	21	3	1.0	2.5	.05	.50	
H	Bal.	20	22	7	1.0	2.0	.02	1.0	W 1.5
I	Bal.	2.5			2.0	31	.30	.50	
J									Zr 99.2
K (304L)	10	Bal.	19		2.0		.03	1.0	
L (304LN)	10	Bal.	19		2.0		.03	1.0	
M (316L)	12	Bal.	17	2.5	2.0		.03	1.0	
N (317L)	13	Bal.	19	3.5	2.0		.03	1.0	
O (904L)	25	Bal.	21	4.5	2.0	1.5	.02	1.0	
P	35	Bal.	20	2.5	2.0	3.5	.07	1.0	
Q	4	Bal.	28	2.0	2.0		.03	.60	
R	5	Bal.	22	3.0	2.0		.03	1.0	
S	5	Bal.	26	3.0	1.5	2.0	.04	1.0	

* Maximum

TABLE 2
CORROSION POTENTIAL IN 3.55% NaCl + 0.1N HCl

Alloy	Ecorr(mV)	Alloy	Ecorr(mV)
F	- 57	N	-121
Q	- 72	P	-145
B	- 77	D	-159
R	- 83	M	-170
H	-100	I	-175
O	-100	E	-272
A	-105	J	-319
C	-109	K	-407
G	-113	L	-414
S	-120		

All potentials are with respect to the saturated calomel reference electrode and are the average of 2 or more runs.

TABLE 3
POLARIZATION RESISTANCE RESULTS IN 3.55% NaCl + 0.1N HCl

Alloy	Rp(ohms)	Icorr(amps)	Corrosion Rate (mpy)
G	180000	1.15E-7	0.05
S	247000	1.23E-7	0.06
Q	240000	1.52E-7	0.07
J	248000	1.89E-7	0.09
H	140000	2.61E-7	0.12
O	150000	2.57E-7	0.12
P	98500	3.08E-7	0.14
R	127000	3.31E-7	0.15
N	131000	3.46E-7	0.16
M	125000	3.47E-7	0.16
B	84000	5.06E-7	0.22
F	90000	5.42E-7	0.24
A	47500	1.11E-6	0.47
C	44000	1.45E-6	0.62
L	6450	3.70E-6	1.69
D	1800	1.01E-5	4.16
I	930	3.00E-5	13.00
E	665	3.68E-5	16.50
K	352	5.80E-5	26.00

TABLE 4
AREA OF HYSTERESIS LOOP WITH 3.55% NaCl + 0.1N HCl

Alloy	Area(Coulombs)	Alloy	Area(Coulombs)
B	2.0	O	7.0
C	2.0	J	9.0
A	2.0	G	9.0
H	2.0	K	12.0
S	3.0	L	14.0
F	3.0	M	15.0
E	4.0	N	17.0
Q	4.0	P	22.0
R	5.0		

TABLE 5
CORROSION POTENTIAL IN 1.0N HCl AND IN 0.1N HCl
(BOTH WITH 3.55% NaCl)

Alloy	Ecorr(mV) 1.0N	Ecorr(mV) 0.1N
H	- 51	-100
F	- 58	- 57
A	- 98	-105
B	-106	- 77
C	-108	-109
O	-328	-100
S	-421	-120
R	-422	- 84
K	-452	-408
Q	-455	- 72

All potentials with respect to the SCE reference

TABLE 6
POLARIZATION RESISTANCE RESULTS IN 3.55% NaCl + 1.0N HCl

Alloy	Rp(ohms)	Icorr(amps)	Corrosion Rate (mpy)
S	43000	2.00E-7	0.09
F	84400	4.62E-7	0.21
H	77500	5.31E-7	0.24
B	61700	7.21E-7	0.31
C	38700	1.32E-6	0.56
A	23800	2.34E-6	1.00
O	257	7.88E-5	36.80
K	167	9.56E-5	43.70
R	79	3.85E-4	180.00
Q	37	9.82E-4	457.00

TABLE 7
CYCLIC POLARIZATION RESULTS
IN 3.55% NaCl + 1.0N HCl

Alloy	Area(Coulombs)	Wt Loss(mg)
H	1.0	0.2
B	1.0	0.3
C	1.0	0.3
A	1.0	0.3
S	2.0	0.4
F	3.0	0.6
O	7.0	1.6
R	2.0	2.8
Q	1.0	6.9

TABLE 8
RESULTS OF EXPOSURE TO 5% SALT FOG PLUS ACID DIPS

	8 weeks + 8 Acid Dips		20 weeks + 20 Acid Dips	
Alloy	Wt Loss(mg)	Corr. Rate(mpy)	Wt Loss(mg)	Corr. Rate(mpy)
B	1.5	.015	0.9	.004
F	2.7	.027	2.5	.010
J	1.2	.016	2.0	.011
C	2.8	.026	3.5	.013
A	2.9	.028	3.7	.014
H	7.1	.073	9.3	.038
D	42.0	.382	154.7	.563
S	93.9	1.045	158.1	.704
O	69.5	.728	179.5	.753
G	85.4	.893	185.8	.778
L	62.0	.605	228.8	.893
R	128.6	1.150	251.8	.900
N	69.9	.752	212.2	.909
K	67.2	.690	226.9	.932
Q	91.6	1.035	207.2	.937
E	91.5	.942	229.8	.947
M	63.1	.673	227.6	.971
P	170.5	1.830	374.6	1.611
I	190.8	1.875	619.6	2.435

TABLE 9
RESULTS OF EXPOSURE TO BEACH CORROSION SITE
PLUS ACID SPRAYS

	60 Days + 5 Sprays		251 Days + 13 Sprays		479 Days + 30 Sprays	
Alloy	Wt. Loss (mg)	Corr. Rate (mpy)	Wt. Loss (mg)	Corr. Rate (mpy)	Wt. Loss (mg)	Corr. Rate (mpy)
B	0.0	.000	0.0	.000	0.0	.000
F	0.0	.000	0.0	.000	0.3	.000
C	0.1	.001	0.1	.001	0.5	.001
A	0.1	.001	0.1	.001	0.7	.001
H	1.5	.014	3.4	.008	3.7	.004
J	0.7	.008	1.4	.004	8.1	.012
S	10.5	.110	13.9	.034	16.3	.021
R	12.1	.099	25.1	.049	37.1	.038
Q	13.0	.139	22.0	.056	35.9	.048
O	14.7	.144	29.3	.069	45.3	.056
G	12.4	.120	28.8	.068	55.5	.069
E	20.3	.195	49.7	.114	81.0	.097
N	18.8	.187	45.0	.107	78.6	.097
M	24.7	.245	56.6	.134	106.2	.132
K	27.7	.278	61.2	.147	113.5	.143
L	34.8	.320	81.6	.177	145.9	.166
D	32.9	.280	106.4	.218	205.1	.220
P	43.1	.435	107.4	.259	222.9	.282
I	95.4	.871	244.7	.534	481.0	.550

SESSION F - OPTICS AND COMMUNICATIONS

Wednesday November 28, 1990

- Digital Codec For Real-Time Processing Of Broadcast-Quality Video Signals
- Recent Advances In Coding Theory For Near-Error-Free Communications
- Microwave Integrated Circuits For Space Applications
- Optical Communications For Space Missions
- Optical Shutter Switching Matrix
- Fiber Optic Tactical Local Area Network (FOTLAN)
- High-Precision Applications Of The Global Positioning System